Physics

Electricity & Magnetism fields

Okayama University *Year* 1995

Practical analysis of 3-D dynamic nonlinear magnetic field using time-periodic finite element method

Takayoshi Nakata
Okayama University

Norio Takahashi
Okayama University

Koji Fujiwara
Okayama University

Kazuhiro Muramatsu
Okayama University

Hiromitsu Ohashi
Okayama University

Hui Ling Zhu
Okayama University

Practical Analysis of 3-D Dynamic Nonlinear Magnetic Field Using Time-Periodic Finite Element Method

Takayoshi Nakata, Norio Takahashi, Koji Fujiwara, Kazuhiro Muramatsu, Hiromitsu Ohashi and Hui Ling Zhu
Department of Electrical and Electronic Engineering, Okayama University, Okayama 700, Japan

***Abstract* — A practical 3-D finite element method using edge elements for analyzing stationary nonlinear magnetic fields with eddy currents in electric apparatus, in which the flux interlinking the voltage winding is given, has been proposed. The method is applied to the analysis of magnetic fields in the Epstein frame.**

I. Introduction

In the practical analysis of periodic magnetic fields with eddy currents in electric machines, the conventional time-stepping method[1] for solving transient phenomena is not effective, because a large number of time steps and very long CPU time are necessary to get the periodic solution. In order to overcome this difficulty, the time-harmonic method[2] is proposed. However, periodic waveform cannot be analyzed precisely taking into account nonlinearity using this method, because the number of harmonics cannot be given beforehand in general. On the other hand, the 3-D time-periodic finite element method[3] using nodal elements has also been developed[4]. The time-periodic waveform can be obtained directly without transient calculation using the relationship between the vector potentials at the instants t and t+T/2 (T : period) of the periodic waveform. However, it takes a long CPU time to solve practical 3-D problems.

In this paper, the 3-D time-periodic FEM is improved by introducing the edge element[5,6] which is more accurate and takes less CPU time than the nodal element[7]. The method is extended to the analysis of the apparatus in which the total flux interlinking the voltage winding is given, and the magnetizing current is unknown. The method is applied to the analysis of the Epstein frame[8].

II. Method of Analysis

A. Fundamental Equations

In the 3-D FEM analysis using edge elements, the residual G_i for the i-th unknown variable is represented as follows[6]:

$$G_i = \iiint_V rot\boldsymbol{N}_i \bullet (\nu\, rot\boldsymbol{A}) dv - \iiint_{V_C} \boldsymbol{N}_i \bullet \boldsymbol{J}_0 dv + \iiint_{V_E} \boldsymbol{N}_i \bullet \sigma \frac{\partial \boldsymbol{A}}{\partial t} dv \tag{1}$$

where $\boldsymbol{A}$ is the magnetic vector potential, $\boldsymbol{J}_0$ is the current density vector in the magnetizing winding, ν and σ are the reluctivity and conductivity, respectively. V, V_C and V_E denote the whole region, the regions for windings and eddy currents, respectively. $\boldsymbol{N}_i$ is the interpolation function defined by the following equation:

$$\boldsymbol{A} = \sum_{i=1}^{nedge} \boldsymbol{N}_i A_i \tag{2}$$

where *nedge* is the number of edges.

When magnetic field distributions in electric machines are analyzed, in which the flux Φ interlinking the voltage winding is given, not only (1) but also the following residual η_k for the k-th voltage winding should be discretized[9,10]:

$$\eta_k = \Phi_k - \iiint_{V_{Bk}} \frac{n_{Bk}}{S_{Bk}} \boldsymbol{A} \bullet \boldsymbol{t}_{Bk} dv \tag{3}$$

where V_{Bk} is the region of the k-th voltage winding. S_{Bk} and n_{Bk} are the cross-sectional area and the number of turns of the voltage winding, respectively. $\boldsymbol{t}_{Bk}$ is the unit tangential vector parallel to the winding direction of the voltage winding.

The current density vector $\boldsymbol{J}_{0l}$ in the l-th magnetizing winding is represented as follows[9]:

$$\boldsymbol{J}_{0l} = \frac{n_{Cl}}{S_{Cl}} I_{0l} \boldsymbol{t}_{Cl} \tag{4}$$

where I_{0l} is the current in the l-th magnetizing winding. The subscript C denotes the magnetizing winding.

B. Nonlinear Analysis

In the nonlinear analysis using the Newton-Raphson iterative technique, the increments of the unknown variables δA_j and δI_{0l} are obtained from the following equation[9]:

$$\begin{bmatrix} \left[\frac{\partial G_i}{\partial A_j}\right] & \left[\frac{\partial G_i}{\partial I_{0l}}\right] \\ \left[\frac{\partial \eta_k}{\partial A_j}\right] & \left[\frac{\partial \eta_k}{\partial I_{0l}}\right] \end{bmatrix} \begin{Bmatrix} \{\delta A_j\} \\ \{\delta I_{0l}\} \end{Bmatrix} = \begin{Bmatrix} -\{G_i\} \\ -\{\eta_k\} \end{Bmatrix} \tag{5}$$

$$(i, j = 1, 2, \cdots, nu)$$
$$(k, l = 1, 2, \cdots, ni)$$

where *nu* is the number of edges with unknown potentials, and *ni* is the number of currents.

As $[\partial G_i / \partial A_j]$ in (5) is the same as that of the conventional finite element method, and the coefficient matrix in this part is symmetric, the other coefficients $[\partial G_i / \partial I_{0l}]$, $[\partial \eta_k / \partial A_j]$ and $[\partial \eta_k / \partial I_{0l}]$ are represented as follows[9]:

$$\frac{\partial G_i}{\partial I_{0l}} = \iiint_{V_{Cl}} \frac{n_{Cl}}{S_{Cl}} \boldsymbol{N}_i \bullet \boldsymbol{t}_{Cl} dv \tag{6}$$

$$\frac{\partial \eta_k}{\partial A_j} = \iiint_{V_{Bk}} \frac{n_{Bk}}{S_{Bk}} \boldsymbol{N}_i \bullet \boldsymbol{t}_{Bk} dv \tag{7}$$

Manuscript received July 6, 1994, revised January 6, 1995. This work was supported in part by the Graint-in-Aid for Scientific Research (B) from the Ministry of Education, Science and Culture in Japan (no.06452201).

$$\frac{\partial \eta_k}{\partial I_{0l}} = 0 \tag{8}$$

The coefficient matrix in (5) is not symmetric, because (6) is different from (7), and some of the diagonal entries become zero as shown in (8). If the voltage winding and the magnetizing winding are assumed to be located at the same position, the coefficient matrix in (5) becomes symmetric. Therefore, the ICCG method can be applied to solve (5). Then, certain numerical values should be added to have non-zero diagonal entries.

C. Selection of Diagonal Value

The value ξ_{iz}, which is added to the zero diagonal entry in the iz-th row, is examined. The following two methods for adding ξ_{iz} are examined:

(a) ξ_{iz} is added only during the process of incomplete Cholesky decomposition (method A).

(b) ξ_{iz} is added to the original coefficient matrix (method B).

Method A has no error in solving the matrix, but method B has an error due to the addition of constant ξ_{iz}.

ξ_{iz} is defined by the following equation:

$$\xi_{iz} = \gamma \bullet \sum_{i=1}^{ncol} \left| H_{iz,i} \right| \tag{9}$$

where $H_{iz,i}$ is the coefficient at the iz-th row and the i-th column in the matrix. *ncol* is the number of columns.

The effects of γ on the number of iterations *niccg* for the ICCG method and the error ε_I due to the modification of the matrix are shown in Fig.1. The error ε_I is defined using the magnetizing currents obtained as follows :

$$\varepsilon_I = \frac{I_B - I_A}{I_A} \tag{10}$$

where I_A and I_B are the magnetizing currents obtained using methods A and B, respectively for linear analysis of the model shown in Fig.3 discussed in section III. When γ is less than 10^{-7}, the calculation is stopped, because the acceleration factor[11] for the ICCG method cannot be determined. When γ is small, *niccg* is reduced in both methods. Therefore, it is preferable to adopt method A with minimum γ, because it is free of errors in solving the matrix equation.

D. Time-Periodic Finite Element Method

When the waveform of a vector potential is symmetric and periodic as shown in Fig.2, the following relationship holds between vector potentials A^t and $A^{t+T/2}$ at the instants t and t+T/2 (T : period):

$$A^t = -A^{t+T/2} \tag{11}$$

The same relationship exists for the current I_0 as follows:

$$I_0{}^t = -I_0{}^{t+T/2} \tag{12}$$

In the time-periodic finite element method, the vector potentials $A^t, A^{t+\Delta t}, ----, A^{t+T/2-\Delta t}$ (Δt : time interval) and currents I^t, $I^{t+\Delta t}$, ----, $I^{t+T/2-\Delta t}$ are treated as unknown

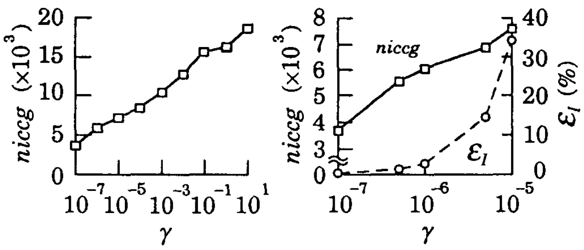

(a) method A (b) method B

Fig. 1 Effect of γ on number of iterations *niccg* for ICCG method and error ε_I.

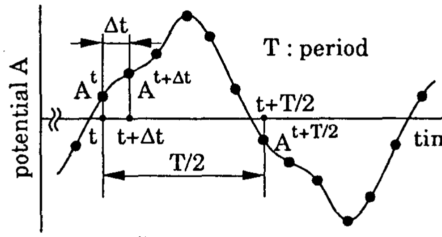

Fig. 2 Periodic waveform.

variables, and they are calculated simultaneously taking into account the relationships of (11) and (12).

When the potential and the current at each instant are treated as unknown variables, the equations for the nonlinear analysis are as follows[3,4]:

$$\left[C^t\right]\begin{Bmatrix}\delta A_j^{t-\Delta t}\\ \delta I_{0l}^{t-\Delta t}\end{Bmatrix} + \left[H^t\right]\begin{Bmatrix}\delta A_j^{t}\\ \delta I_{0l}^{t}\end{Bmatrix} = \begin{Bmatrix}-\{G_i^t\}\\ -\{\eta_k^t\}\end{Bmatrix}$$

$$\left[C^{t+\Delta t}\right]\begin{Bmatrix}\delta A_j^{t}\\ \delta I_{0l}^{t}\end{Bmatrix} + \left[H^{t+\Delta t}\right]\begin{Bmatrix}\delta A_j^{t+\Delta t}\\ \delta I_{0l}^{t+\Delta t}\end{Bmatrix} = \begin{Bmatrix}-\{G_i^{t+\Delta t}\}\\ -\{\eta_k^{t+\Delta t}\}\end{Bmatrix}$$

$$\bullet$$
$$\bullet$$
$$\bullet$$

$$\left[C^{t+T/2-\Delta t}\right]\begin{Bmatrix}\delta A_j^{t+T/2-2\Delta t}\\ \delta I_{0l}^{t+T/2-2\Delta t}\end{Bmatrix} + \left[H^{t+T/2-\Delta t}\right]\begin{Bmatrix}\delta A_j^{t+T/2-\Delta t}\\ \delta I_{0l}^{t+T/2-\Delta t}\end{Bmatrix} = \begin{Bmatrix}-\{G_i^{t+T/2-\Delta t}\}\\ -\{\eta_k^{t+T/2-\Delta t}\}\end{Bmatrix} \tag{13}$$

where $[C]$ and $[H]$ are the same as those of the conventional time-stepping method[1,6].

By applying the relationships of (11) and (12) to $\{\delta A_j^{t-\Delta t}\}$ and $\{\delta I_{0l}^{t-\Delta t}\}$ in (13), the following matrix equation is obtained:

$$\begin{bmatrix} [H^t] & 0 & \cdots & 0 & -[C^t] \\ [C^{t+\Delta t}] & [H^{t+\Delta t}] & \cdots & 0 & 0 \\ \vdots & \vdots & & \vdots & \vdots \\ \vdots & \vdots & & \vdots & \vdots \\ 0 & 0 & \cdots & [C^{t+T/2-\Delta t}] & [H^{t+T/2-\Delta t}] \end{bmatrix}$$

$$\times\begin{Bmatrix} \begin{Bmatrix}\{\delta A_j^t\} \\ \{\delta I_{0l}^t\}\end{Bmatrix} \\ \begin{Bmatrix}\{\delta A_j^{t+\Delta t}\} \\ \{\delta I_{0l}^{t+\Delta t}\}\end{Bmatrix} \\ \vdots \\ \vdots \\ \begin{Bmatrix}\{\delta A_j^{t+T/2-\Delta t}\} \\ \{\delta I_{0l}^{t+T/2-\Delta t}\}\end{Bmatrix} \end{Bmatrix} = \begin{Bmatrix} \begin{Bmatrix}-\{G_i^t\} \\ -\{\eta_k^t\}\end{Bmatrix} \\ \begin{Bmatrix}-\{G_i^{t+\Delta t}\} \\ -\{\eta_k^{t+\Delta t}\}\end{Bmatrix} \\ \vdots \\ \vdots \\ \begin{Bmatrix}-\{G_i^{t+T/2-\Delta t}\} \\ -\{\eta_k^{t+T/2-\Delta t}\}\end{Bmatrix} \end{Bmatrix} \quad (14)$$

As the coefficient matrix in (14) is very large, considerably long CPU time and large computer memory are required for the conventional method of solution. Therefore, an iterative technique is introduced by dividing (14) into the following equations[3]:

$$\left[\boldsymbol{H}^{t+m\Delta t}\right]\begin{Bmatrix}\delta A_j^{t+m\Delta t} \\ \delta I_{0l}^{t+m\Delta t}\end{Bmatrix} = -\alpha \bullet \beta_m\left[\boldsymbol{C}^{t+m\Delta t}\right]\begin{Bmatrix}\delta A_j^{t+(m-1)\Delta t} \\ \delta I_{0l}^{t+(m-1)\Delta t}\end{Bmatrix} + \begin{Bmatrix}-\{G_i^{t+m\Delta t}\} \\ -\{\eta_k^{t+m\Delta t}\}\end{Bmatrix} \quad (15)$$

$$(m = 0, 1, \cdots, ns-1)$$

where ns is the number of time steps in half a period. β_m is equal to -1 (m=0) and 1 (m≠0). α is the relaxation factor[3] and is chosen to be zero, because minimum modification is required in the software for the time-stepping method. Although α is chosen to be zero, the relationship of (11) is considered in the second term of the right-hand side of (15). The nonlinear iterations are carried out in the outer loop of the time step iterations[4] until A and I_0 converge. Using this iterative technique, the nonlinear steady-state magnetic fields can be obtained within shorter CPU time than the time-stepping method[4] in which the nonlinear iteration is carried out at each step from the transient state to the steady state.

III. Application

A. Analyzed Model

The Epstein frame[8] which is shown in Fig.3 is chosen as the analyzed model. The specimen is highly grain-oriented silicon steel (AISI:M-2H, thickness:0.35mm). The interlaminar gap between specimens at the corner is assumed to be 0.011mm (space factor : 97%). The magnetizing winding is excited so that the average value Bm of the maximum flux density in the specimens can be set at 1.7T. The waveform of the flux is sinusoidal, and the frequency is 50Hz.

In order to simplify the analysis, the model is modified as follows:

(a) In order to apply the ICCG method, the position of the voltage winding is assumed to be located at the same position of the magnetizing winding, so that the matrix can be symmetrical. This is because the flux in the air is very small compared with that in the specimens.

(b) In order to reduce the analyzed region, it is assumed that the number of stacked specimens is infinite.

(c) The hysteresis is neglected. Only saturation is taken into account.

B. Results and Discussion

Fig.4 shows the waveforms of the average flux density interlinking the specimens and the ampere-turns of the magnetizing winding in the cases of with and without eddy currents. Half a period of the waveform is divided into 6 steps, namely Δt=1.67ms, because extremely long CPU time is necessary. When the flux is increased, the magnetizing current obtained by the analysis taking into account the eddy currents is larger than that without eddy currents, due to the additional magnetizing current that is needed in the case of the presence of eddy currents. The figure shows that the result obtained from the new software is theoretically acceptable.

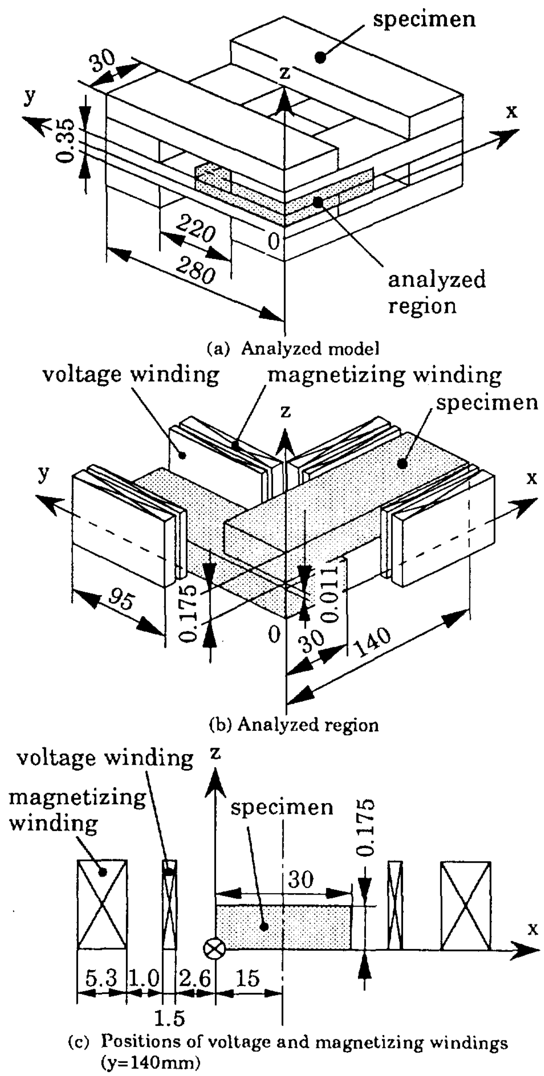

(a) Analyzed model

(b) Analyzed region

(c) Positions of voltage and magnetizing windings (y=140mm)

Fig. 3 Analyzed model.

Table I shows the discretization data and the CPU time for this analysis. The number of nonlinear iterations for the analysis with eddy currents is not so much different from that without eddy currents. However, the CPU time for the analysis with eddy currents is much longer than that without eddy currents due to the difference of convergence characteristics for the ICCG method. The CPU time for the new method is compared with the conventional method (time-stepping method, nodal element) in [4,7], because the conventional method cannot be applied to this model due to extremely long CPU time. Our results in the references show that the CPU time of the new method is shorter than the conventional methods as follows:

(a) The CPU time for the analysis using the time-stepping method is 3 times longer than that using the time-periodic method[4].
(b) The CPU time required for the nodal element analysis is 6 times longer than that by the edge element in the eddy currents model proposed by the Institute of Electrical Engineers of Japan[7].

Therefore, the time-periodic finite element method should be applied in the analysis of such an Epstein frame, because the CPU time for the conventional method is about 18 times longer than that in the new method.

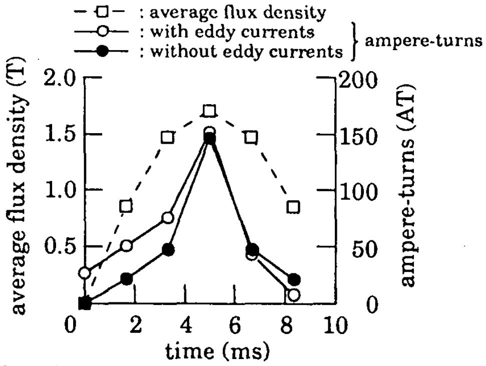

Fig. 4 Waveforms of average flux density and ampere-turns.

TABLE I
Discretization data and CPU time

model	without eddy currents	with eddy currents
number of elements *1	14,112	
number of nodes	16,641	
number of unknowns	38,809	
number of non-zeros	600,024	
memory requirement (MB)	15.5	17.4
number of nonlinear iterations *2	8*3(13*4)	13
number of iterations for ICCG method *5	13,009	1,077,951
total CPU time (h) *6	1.9	146.5

*1 element type : 1st–order brick edge element
*2 convergence criterion for Newton–Raphson method : 0.01T
*3 average number of nonlinear iterations in 5 steps
*4 maximum number of nonlinear iterations in 5 steps
*5 convergence criterion for ICCG method : 10^{-5}
*6 computer used : IBM workstation 37T (25.9 MFLOPS)

IV. Conclusions

A practical 3-D finite element method for analyzing the stationary magnetic fields in electric apparatus is proposed. The method is applied to the analysis of the magnetic field in the Epstein frame. The results obtained can be summarized as follows:

(1) The 3-D time-periodic finite element method using edge elements is developed. The CPU time can be considerably reduced compared with that in the conventional time-stepping method using nodal elements.
(2) The method of analysis in which the flux Φ interlinking the voltage winding is given, is developed. If the voltage and magnetizing windings can be assumed to be located at the same position, the coefficient matrix becomes symmetrical. During the incomplete Cholesky decomposition required for the ICCG method, the minimum value at which the acceleration factor can be obtained, should be added in order to set non-zero diagonal entries.
(3) The magnetic fields in the Epstein frame which are theoretically acceptable, are obtained within practical CPU time.

The effects of eddy currents on the magnetic path length of the Epstein frame will be investigated in the future. The detailed investigation of the effect of number of time steps on the CPU time and accuracy will be reported in the future.

References

[1] T.Nakata and Y.Kawase, "Numerical analysis of nonlinear transient magnetic field using the finite element method," *Journal of IEE, Japan*, vol. 104-B, no. 6, pp. 380-386, June 1984.
[2] R.Albanese, E.Coccorese, R.Martone, G.Miano and G.Rubinacci, "Periodic solutions of nonlinear eddy current problems in three-dimensional geometries," *IEEE Trans. Magn.*, vol. 28, no. 2, pp. 1118-1121, March 1992.
[3] T.Hara, T.Naito and J.Umoto, "Field analysis of corona shield region in high voltage rotating machines by time-periodic finite element method," *Journal of IEE, Japan*, vol. 102-B, no. 7, pp. 423-430, July 1982.
[4] T.Nakata, N.Takahashi, K.Fujiwara and A.Ahagon, "3-D non-linear eddy current analysis using the time-periodic finite element method," *IEEE Trans. Magn.*, vol. 25, no. 5, pp. 4150-4152, September 1989.
[5] A.Kameari, "Calculation of transient 3D eddy current using edge-elements," *ibid.*, vol. 26, no. 2, pp. 466-469, March 1990.
[6] K.Fujiwara, "3-D magnetic field computation using edge element (invited)," *Proceedings of the 5th IGTE Symposium on Numerical Field Calculation in Electrical Engineering*, pp. 185-212, September 1992.
[7] T.Nakata, N.Takahashi, K.Fujiwara, K.Muramatsu and T.Imai, "Comparison of various methods of analysis and finite elements in 3-D magnetic field analysis," *IEEE Trans. Magn.*, vol. 27, no. 5, pp. 4073-4076, September 1991.
[8] IEC (International Electrotechnical Commission) 404-2, "Method of measurement of the magnetic properties of magnetic sheet and strip by means of an Epstein frame," 1994.
[9] T.Nakata, N.Takahashi, K.Fujiwara and A.Ahagon, "3-D finite element method for analyzing magnetic fields in electrical machines excited from voltage sources," *IEEE Trans. Magn.*, vol. 24, no. 6, pp. 2582-2584, November 1988.
[10] S.Bouissou and F.Piriou, "Study of 3-D formulations to model electromagnetic devices," *ibid.*, vol. 30, no. 5, pp. 3228-3231, September 1994.
[11] K.Fujiwara and T.Nakata, "Automatic determination of acceleration factor for the ICCG method," *ibid.*, vol. 31, no. 3, May 1995.